Design of 100-V Super-Junction Trench Power MOSFET with Low On-Resistance

Young Hwan Lho and Yil-Suk Yang

Power metal-oxide semiconductor field-effect transistor (MOSFET) devices are widely used in power electronics applications, such as brushless direct current motors and power modules. For a conventional power MOSFET device such as trench double-diffused MOSFET (TDMOS), there is a tradeoff relationship between specific on-state resistance and breakdown voltage. To overcome the tradeoff relationship, a super-junction (SJ) trench MOSFET (TMOSFET) structure is studied and designed in this letter. The processing conditions are proposed, and studies on the unit cell are performed for optimal design. The structure modeling and the characteristic analyses for doping density, potential distribution, electric field, width, and depth of trench in an SJ TMOSFET are performed and simulated by using of the SILVACO TCAD 2D device simulator, Atlas. As a result, the specific on-state resistance of 1.2 mΩ-cm^2 at the class of 100 V and 100 A is successfully optimized in the SJ TMOSFET, which has the better performance than TDMOS in design parameters.

Keywords: Super-junction MOSFET, power MOSFET, trench MOSFET, on-state resistance, breakdown voltage.

I. Introduction

Super-junction (SJ) metal-oxide semiconductor field-effect transistor (MOSFET) power devices are well known for lower on-state resistance and gate charge. However, it is difficult to fabricate the exact balanced doping profile, and the impact of imbalance results in varying breakdown voltages (BVs). For the conventional MOSFET device structure, there exists a tradeoff relationship between specific on-state resistance and BV. In this letter, an SJ trench MOSFET (TMOSFET) structure is proposed to overcome the specific on-resistance occurred in the drift region (see Fig. 1). The BV is very sensitive to the doping concentration [1]. The SJ structure was applied to reduce the specific on-resistance of high-voltage power MOSFET and the trench gate MOSFET for lower voltage in the past, but the technology trend of lowering the specific on-resistance has been developed to apply the combined SJ and trench structure of power MOSFET with the BV below 200 V.

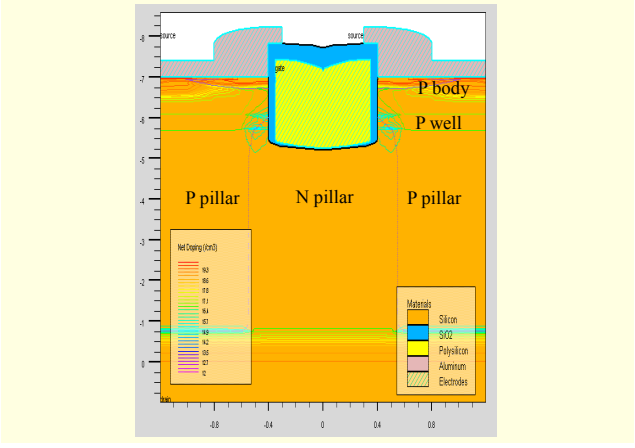

Fig. 1. Fundamental structure of SJ TMOSFET.

II. Device Structure and Theoretical Analyses

1. On-Resistance of Power SJ MOSFET

A much higher doping concentration can be applied in the drift region of the power SJ MOSFET structure when compared with the non-SJ structures. The increased doping

Manuscript received June 8, 2011; revised July 19, 2011; accepted July 28, 2011.
This work was supported by the IT R&D program of MKE/KEIT [10035171].
Young Hwan Lho (phone: +82 42 629 6731, yhlho@wsu.ac.kr) is with the Department of Railroad Electricity and Information Communications, Woosong University, Daejeon, Rep. of Korea.
Yil-Suk Yang (ysyang@etri.re.kr) is with the Convergence Components & Materials Research Laboratory, ETRI, Daejeon, Rep. of Korea.
http://dx.doi.org/10.4218/etrij.12.0211.0251

concentration in the drift region enables a dramatic reduction of the drift region resistance for the required BV. The lower specific on-resistance can be achieved by removing the junction FET region [2]. The drift region resistance is composed of the two components, R_{D1} for the N-type drift region and R_{D2} for the substrate [3]. For high-voltage power SJ MOSFET structures, the contribution from the N-type drift region is much higher than that from the N buffer layer.

The ideal specific on-resistance [3] for the SJ devices is

$$R_{ON,SP} = \frac{BV}{\varepsilon_S \mu_N E_{CU}^2}\left(\frac{W_N + W_P}{2}\right), \quad (1)$$

where ε_S is the dielectric constant, μ_N is the electron mobility, E_{CU} is the critical electrical field, and W_N and W_P are the widths in N-type and P-type drift regions, respectively. The E_{CU} [3] is

$$E_{CU} = 5.53 \times 10^5 V_{BR}^{-1/6}. \quad (2)$$

Substituting (2) into (1) leads to

$$R_{ON,SP} = \frac{1.635 \times 10^{-12} BV^{4/3}(W_N + W_P)}{\varepsilon_S \mu_N}. \quad (3)$$

Since the same width for the P-type and N-type drift regions in SJ devices is commonly used, the charge balance should be kept.

The on-resistance can be obtained by currents flowing from the channel between the source and the drain electrodes as

$$R_{ON}=R_{CS}+R_N+R_{CH}+R_{D1}+R_{D2}+R_{CD}, \quad (4)$$

where R_{CS} is the source contact resistance, R_N is the source resistance, R_{CH} is the channel resistance, and R_{CD} is the drain contact resistance.

Figure 2 gives the various components that are applied for the analysis of the on-resistance. Here, W_N is the width of the N-type drift region and W_P is the width of the P-type drift region.

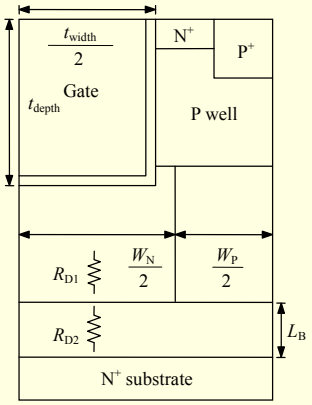

Fig. 2. Structure of power SJ TMOSFET.

2. Channel Resistance ($R_{CH,ON}$)

The value of the specific on-resistance from the channel in the SJ MOSFET structure is smaller than that of the power double-diffused MOSFET structure due to the shorter channel length and cell pitch. The specific on-resistance [3] made by the channel in the power SJ MOSFET structure is

$$R_{CH,SP} = \frac{L_{CH} W_{cell}}{2\mu_{Ni} C_{OX}(V_G - V_{TH})}, \quad (5)$$

where L_{CH} is the channel length, W_{cell} is the width of unit cell, μ_{Ni} is the channel electron mobility, C_{OX} is the channel gate capacitance, V_G is the gate voltage, and V_{TH} is the threshold voltage.

3. Drift Region Resistance (R_D)

The resistances in the drift region consist of $R_{D1,SP}$ and $R_{D2,SP}$ as shown below:

$$R_{D1,SP} = \frac{L_D - t_{trench}}{q\mu_N N_D W_N} W_{cell}, \quad (6)$$

$$R_{D2,SP} = \frac{L_B}{q\mu_N N_D W_N} W_{cell}, \quad (7)$$

where L_D is the length of the drift region, t_{trench} is the trench depth, W_{cell} is the cell width, q is the charge, N_D is the doping density of the drift region, and W_N is the width of N pillar.

4. Total Resistance

The total on-resistance for the power SJ MOSFET structure is computed by combing the channel on-resistance and the drift region on-resistance while neglecting the contact and source resistances in (4) as follows:

$$R_{ON,SP}=R_{CH,SP}+R_{D,SP}. \quad (8)$$

The ideal specific on-resistance for a drift region is given by

$$R_{IDEAL,SP} = \frac{W_{PP}}{q\mu_N N_D}, \quad (9)$$

where W_{PP} is the depletion width at BV of PN junction, and N_D is the doping concentration of the drift region. The sheet resistance, the pillar widths of P and N, and the on-resistance in the drift region are important factors in designing the vertical power SJ TMOSFET.

For the case of the BV of 120 V considering a 20% margin of 100 V, the drift doping concentration, the width of N/P pillar (W_N and W_P), and the epi-thickness suggested in Baliga's design parameters [3] are found to be $2.15 \times 10^{16}/cm^3$, 1.5 μm, and 4.5 μm, respectively.

III. Simulations and Discussion

The doping concentration in the drift region of the power SJ MOSFET structure should be optimized to obtain the desired BV. The doping concentration for N-type and P-type drift regions are assumed to be equal. In the manufacturing field [4], it is difficult to make the doping concentration exactly equal, and the impact of imbalance results in varying BVs. The surface structure in TMOSFET is shown in Fig. 3, and the process flow fabricating self-aligned TMOSFET is proposed in [5].

Figure 3 shows the TMOSFET, which is implemented based on the self-align trench double-diffused MOSFET (TDMOS) process [5] developed at ETRI. In designing the vertical SJ TDMOS, the applied parameters are the P well junction depth of 1.2 μm, the unit cell width of 2.4 μm, each N and P pillar width of 1.2 μm, and the epi-thickness of 8 μm. Here, the electric field at the point of breakdown has to be kept below E_{CU} of 2.5×10^5 V/cm required to create the BV.

The resistance contributions from the N^+ substrate and the contacts are neglected during the simulation. The device parameters applied to each blocking voltage are given in Table 1. The cell density is increased by reducing the trench width, which leads to a decrease in the channel resistance, and the gate capacitance is increased.

The SJ TMOSFET structure and the doping concentration in the vertical direction of P pillar are shown in Figs. 4(a) and 4(b), respectively. The doping profile at the boundary between the substrate and the drift region is determined by the out-diffusion of substrate layer during forming the P well.

Figures 5(a) to 5(d) represent the distribtutions for the electric potential, current flow line, ionization coefficients, and electric field at BV of 120 V, respectively. The potential in Fig. 5(a) remains constant as the drain voltage increases. The current distribution curve mostly appears in N/P pillar region as shown in Fig. 5(b). Figure 5(c) shows the ionization coefficients which affect the BV directly. The electric field is concentrated at the corner of trench region in the conventional power MOSFET, which forces the BV to be lower. It is important to make the electric field of Fig. 5(d) with less value wider since the ionization coefficients are related to the electric distribution.

The specific on-resistance of measured data shown in Fig. 6 [6] is about 1.4 mΩ·cm^2 for TDMOS without an SJ structure, and the value cannot be applicable to brushless direct current (BLDC) motor since it requires $R_{ON,SP}$ of less than 1.2 mΩ·cm^2

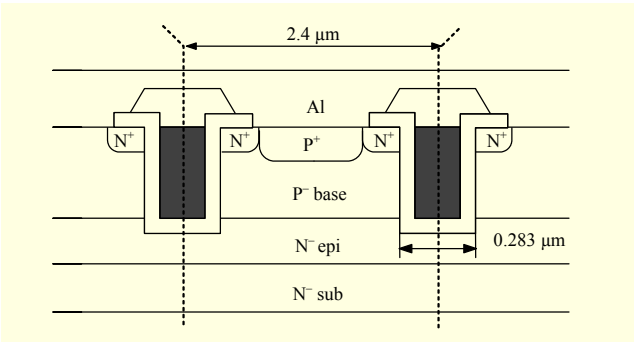

Fig. 3. Surface structure of TMOSFET.

Table 1. Main characteristics of TDMOS and SJ TMOSFET.

Device parameter		TDMOS	SJ TMOSFET
Cell pitch		2.4 μm	
Substrate dopant ρ		As 1 mΩ·cm to 5 mΩ·cm	
Epi. structure	Thickness	8 μm	
	N^- epi concentration	2.5×10^{15}/cm^3	1×10^{16}/cm^{3*}
Thickness, t_{OX}		500 Å	
$X_{j-P\ well}$		1.2 μm to 1.3 μm	
Trench depth Trench width		1.75 μm 0.283 μm	
N^+ source		0.5 μm	
P^+ body contact		1.5 μm	

*: N^- epi concentration is for each N and P pillar.

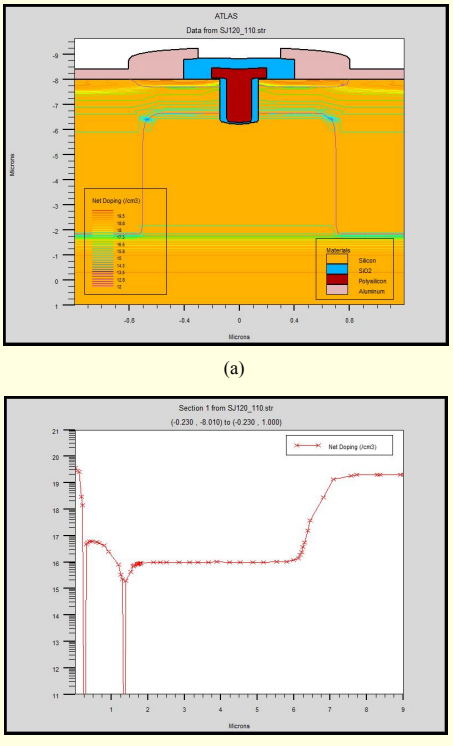

Fig. 4. (a) SJ TMOSFET structure and (b) doping concentration at vertical direction of P pillar.

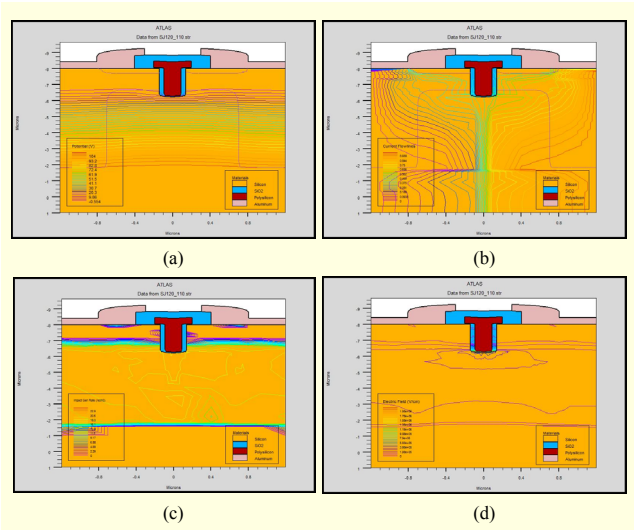

Fig. 5. Distributions at BV (V_{drain}=120 V): (a) electric potential, (b) current flow, (c) ionization coefficients, and (d) electric field.

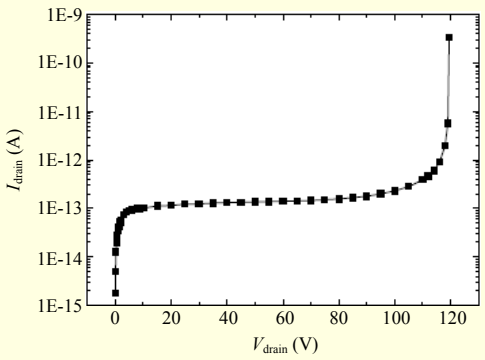

Fig. 6. Current-voltage characteristics at BV=120 V.

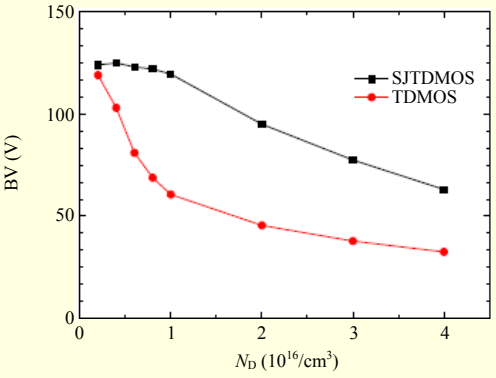

Fig. 7. Pillar doping concentration vs. BV.

for the project being under the development at ETRI. The difference between the simulated value and the experimental one is originated from the contact resistances of drain and source.

Figure 6 shows the BV at 120 V, and Fig. 7 represents pillar doping concentration versus BV. When the length of the drift region is 8 μm and the doping concentration is 2.5×10^{15} in TDMOS, the BV is obtained 119 V and the specific on-resistance is 1.12 mΩ·cm^2 in simulation. To get the same BV at SJ structure, the doping concentration of the pillar required is 1×10^{16}, and $R_{ON,SP}$ is reduced to 0.7 mΩ·cm^2 in simulation. Then, it is expected that the improved specific on-resistance is applicable to BLDC motor with enough margin. Here, the simulation result for the pillar concentration meets the BV of 120 V shown in Baliga's design parameters [2].

IV. Conclusion

The specific on-state resistance of 1.2 mΩ·cm^2 at the class of 100 V and 100 A is successfully optimized by using SJ TMOSFET, showing better performance than TDMOS. First, the specific on-state resistance mainly depends on the ideal pillar width and concentration. Second, the fundamental structure of trench gate SJ MOSFET is designed, and the doping concentration of pillar, potential distribution, current, ionization coefficients, and electric field are analyzed after simulation by SILVACO TCAD [7]. It is determined that the design of the unit cell in this letter can be applied to the implementation of the SJ TMOSFET for a chip in BLDC motor with enough margin when the implementation is done.

References

[1] Y. Chen, Y.C. Liang, and G.S. Samudra, "Design of Gradient Oxide-Bypassed Super-Junction Power MOSFET Devices," *IEEE Trans.*, vol. 22, no. 4, July 2007, pp. 1303-1309.

[2] Y. Wang et al., "Gate Enhanced Power UMOSFET with Ultralow On-Resistance," *IEEE Electron. Device Lett.*, vol. 31, no. 4, Apr. 2010, pp. 338-340.

[3] B.J. Baliga, *Advanced Power MOSFET Concepts*, New York Springer-Science, 2010, pp. 323-354.

[4] J.A. Yedinack et al., "Super-Junction Structures and Fabricating Methodologies for Power Devices," Korean Patent: 10-2010-0083153.

[5] J. Kim et al., "A Novel Technique for Fabricating High Reliable Trench DMOSFETs Using Self-Align Technique and Hydrogen Annealing," *IEEE Trans. Electron Devices*, vol. 50, no. 2, 2003, pp. 378-383.

[6] S.-G. Kim et al., "High-Density Nano-Scale N-Channel Trench-Gated MOSFETs Using the Self-aligned Technique," *J. Korean Physical Society*, vol. 57, no. 4, Oct. 2010, pp. 802-805.

[7] SILVACO TCAD Manual, Atlas, 2011.